DESIGN OF REC PERMANENT MAGNET QUADRUPOLES TAKING INTO ACCOUNT B, H NON-LINEARITY*

Robert L. Gluckstern
University of Maryland at College Park

Ronald F. Holsinger
Field Effects, Inc., Carlisle, Mass.

Summary

Most Rare Earth Cobalt (REC) materials have linear behavior of $B_{||}$ vs $H_{||}$ with permeability about 1 over a wide range of $H_{||}$. However some of the materials with high magnetization become non-linear in the 2nd quadrant of the B-H space, while others with lower magnetization depart from linearity in the 3rd quadrant. Since the normal quadrupole design will drive many segments into the second quadrant and some even into the 3rd quadrant, the non-linear behavior of $B_{||}$ vs $H_{||}$ can distort the quadrupole field usually desired. Calculations have been performed using the computer code PANDIRA to explore the magnitude of the distortion caused by these non-linearities. In this paper, the usual quadrupole design is modified to use segments of lower magnetization but greater linearity in those places where segments are driven magnetically into the 2nd and 3rd quadrants. Prescriptions are given for the opening wedge angle and easy axis orientation of each segment which lead to the vanishing of the unwanted multipole components. Clearly the resulting purity of the quadrupole field comes at the expense of achieving the greatest field strength. Similar geometrical modifications can be used for other multipole designs. These techniques apply direction to the dependence on aximuthal angle for both the 2-D and 3-D multipole designs. These principles have been applied to a specific design problem.

I. Introduction

Rare earth cobalt (REC) materials are being used to build high field permanent magnets for a variety of applications. Among these are the use of REC quadrupoles to focus particle beams, higher order multipoles to provide compensation for non-linearities, and an array of dipoles to generate synchrotron radiation in wigglers and undulators.[1]

In some of the applications the primary goal is maximum field strength. In others it is maximum field purity (absence of undesired multipoles). On some occasions, both maximum field strength and purity are desired. Unfortunately, those materials which have the highest magnetization have B-H curves which are not linear over the full desired range and may even have values of $\mu_{||}$ and $\mu_{\perp}$ which are significantly different from unity. As a result, the field may have large multipole impurities.

The purpose of this paper is to explore these impurities for two dimensional quadrupoles, and to devise design principles using two different materials which provide minimum impurities and maximum field gradient. These principles will then be applied to a specific design problem.

II. Basic Quadrupole Design

A. Continuous Easy Axis Rotation

The basic 2-D quadrupole is one which consists of a ring of REC material magnetized via a pattern where the easy axis orientation is at an angle 3θ, where r, θ are the conventional 2-D polar coordinates. For the case where $\mu_{||} = \mu_{\perp} = 1$, it is easy to show that the interior field is a pure quadrupole field, with maximum field at the bore given by

$$B^{max} = 2M(1 - \frac{a}{b}) \qquad (2.1)$$

where a/b is the ratio of inner to outer radius of the ring, and M is the magnitude of the magnetization.

B. Segmented Ring

Practical designs consist of N arc or trapezoidal segments of identical shape magnetized in a j^{th} pattern where the easy axis orientation for the j^{th} segment is at an angle $3\theta_j$, where θ_j is the central azimuthal angle of the j^{th} segment. Such an arrangement for 8 touching segments is shown in Figure 1.

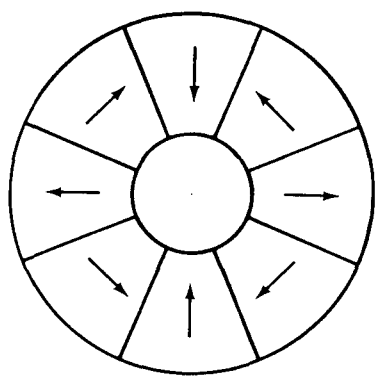

Fig. 1 Eight Segment REC Quadrupole Magnet Configuration

In this case the maximum quadrupole field at the bore is reduced by the form factor

$$\frac{\sin\frac{3\pi}{8}}{\frac{3\pi}{8}} \simeq 0.78 \qquad (2.2)$$

and selected higher multipoles (10, 18, 26, ...) are also present.

In order to understand the range of values to which B and H are extended in a typical design, it is simplest to examine the 2-D ring with $\mu_{||} = \mu_{\perp} = 1$

[1] K. Halbach, Nucl. Instr. and Meth. 169, 1(1980); R. F. Holsinger, Proc. of 1979 Linac Conference, Montauk Point, N.Y., p. 373; K. Halbach. Nucl. Instr. and Meth. 187, 109 (1981).

*Computations supported by Los Alamos National Lab.

and continuous easy axis rotation. In this case one writes

$$\vec{B} = \vec{H} + \vec{M} \quad , \quad \nabla \cdot \vec{B} = 0$$
$$\nabla \times \vec{H} = 0 \quad , \quad \vec{H} = \nabla\Phi \qquad (2.3)$$
$$\nabla^2\Phi = - \nabla \cdot \vec{M}$$

For $a < r < b$,

$$M_r = M \cos 2\theta \qquad \nabla \cdot \vec{M} = \frac{3M\cos 2\theta}{r}$$
$$M_\theta = M \sin 2\theta \quad , \qquad (2.4)$$

Satisfying the boundary conditions which make H_{tan} and B_{normal} continuous, one finds within the REC ring

$$B_{11}/M = \cos^2 2\theta\left(2 - \frac{2r}{b}\right) + \sin^2 2\theta\left(\frac{2r}{b} - 1\right)$$
$$H_{11}/M = \cos^2 2\theta\left(1 - \frac{2r}{b}\right) + \sin^2 2\theta\left(\frac{2r}{b} - 2\right) \qquad (2.5)$$

For $r = a$, H_{11}/M extends from $-2 + 2\frac{a}{b}$ at $\theta = \frac{\pi}{4}$ to $1 - 2\frac{a}{b}$ at $\theta = 0$. For $a \ll b$, this corresponds to a range of H_{11} from -2M to + M, well beyond the limits of linearity for the maximum field materials, such as that shown in Figure 2.

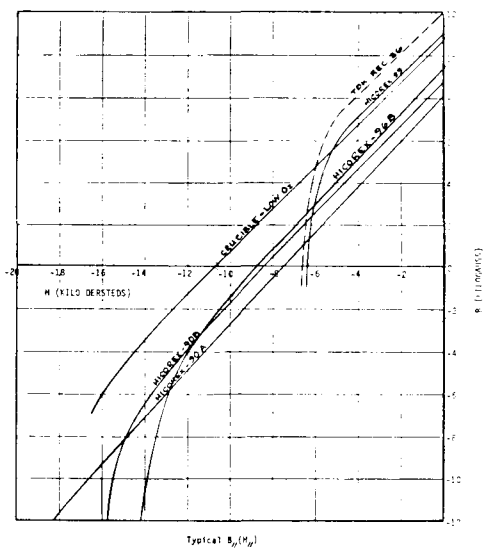

Fig. 2 B(H) Curves for Different REC Materials

III. Factors Contributing to Multipole Impurities

A. Permeability Greater than Unity

Most REC materials have permeabilities in the range from 1.03 to 1.20. If the permeability is the same parallel to and perpendicular to the easy axis, the formulation in the preceding section is easily modified, and the magnetic field multipole strengths are each modified by a factor proportional to $\mu - 1$. No new multipoles are introduced in the case of the continuous easy axis rotation, and therefore the practical consequence is that the quadrupole strength is reduced by the factor

$$\frac{2}{\mu+1} \simeq 1 - \frac{\mu-1}{2} \qquad (3.1)$$

for μ close to 1. For the ring with eight segments, new multipoles with strengths proportional to $(\mu-1)$ are introduced for n=6, 14, 22, ...

B. Permeability Greater than Unity Along Easy Axis

The analysis is considerably more complex if $\mu_{11} \neq \mu_\perp$. If we set $\mu_\perp = 1$,* and $\mu_{11} = 1 + \delta$, where $\delta \ll 1$, we can write

$$\nabla \times \vec{H} = 0 \quad , \quad \vec{H} = \nabla\Phi$$
$$\vec{B} = \vec{H} + \delta\vec{H}_{11} + \vec{M} \quad , \quad \nabla \cdot \vec{B} = 0$$
$$\nabla^2\Phi = - \nabla\cdot\vec{M} - \delta\, \nabla\cdot\vec{H}_\mu \qquad (3.2)$$

For small δ, we can solve this equation to first order in δ by setting H_{11} to be the solution obtained for the continuous ring for $\mu = 1$. (The segmented ring introduces additional complications which are not important in the present analysis.)

If we write

$$|H_{11}| = \frac{\vec{H}\cdot\vec{M}}{g} = \cos 2\theta\, H_r + \sin 2\theta\, H_\theta \qquad (3.3)$$

we can obtain the components of the H_{11} as

$$(H_{11})_r = \cos^2 2\theta\, H_r + \cos 2\theta \sin 2\theta\, H_\theta$$
$$(H_{11})_\theta = \cos 2\theta \sin 2\theta\, H_r + \sin^2 2\theta\, H_\theta. \qquad (3.4)$$

from which we obtain

$$\nabla\cdot\vec{H}_{11} = \frac{1}{r}\frac{\partial}{\partial r} r[\cos^2 2\theta\, H_r + \cos 2\theta \sin 2\theta\, H_\theta]$$
$$+ \frac{1}{r}\frac{\partial}{\partial\theta}[\cos 2\theta \sin 2\theta\, H_r + \sin^2 2\theta\, H_\theta] \qquad (3.5)$$

Analysis of the continuous ring for $\mu = 1$ leads to the unperturbed fields within the ring

$$H_o = \nabla\Phi_o, \quad \Phi_o = M\cos 2\theta\left(r - \frac{r^2}{b}\right) \qquad (3.6)$$

which eventually leads to

$$\nabla\cdot\vec{H}_{11} = -\frac{9}{4r} M\cos 2\theta + \left(\frac{21}{4r} - \frac{8}{b}\right) M\cos 6\theta \qquad (3.7)$$

If we now solve equation (3.2) by matching fields in the regions $0 \le r \le a$, $a \le r \le b$, $b \le r$, we obtain a quadrupole field at the bore modified by the factor

$$1 - \frac{\delta}{2} \qquad (3.8)$$

as well as a new multipole field (n=6) of strength

$$B_6^\delta(a) = \delta M\left[\frac{9}{10} - \frac{3a}{2b} + \frac{3a^5}{5b^5}\right] \qquad (3.9)$$

For $\frac{a}{b} = \frac{1}{3}$, this has the approximate value

$$B_6(a) \simeq .402\,\delta M \qquad (3.10)$$

It is clear from the form of the analysis, that in a ring with N segments, additional multipoles with strength proportional to δ will be introduced of order n = N-2, 2N-2, 3N-2, ... as in

*The effect of having both μ_{11} and $\mu_\perp$ different from one produces a result approximately equivalent to that described in Section IIIA supplemented by a correction proportional to $\mu_{11} - \mu_\perp$, which is calculated in this section by setting $\mu_{11} - \mu_\perp = \delta$. In this case, for convenience we have set $\mu_\perp = 1$, $\mu_{11} = 1 + \delta$.

the $\mu_{\parallel} = \mu_{\perp} \neq 1$ case, and n = 6, N ± 6, 2N ± 6, ---, the first of which is specified in Equations (3.9) and (3.10). In addition, the terms proportional to δ in Equations (3.8), (3.9) and (3.10) will be modified further for a segmented ring.

IV. Compensated Ring

Let us consider a ring with eight touching segments made of two different materials, as shown in Figure 3

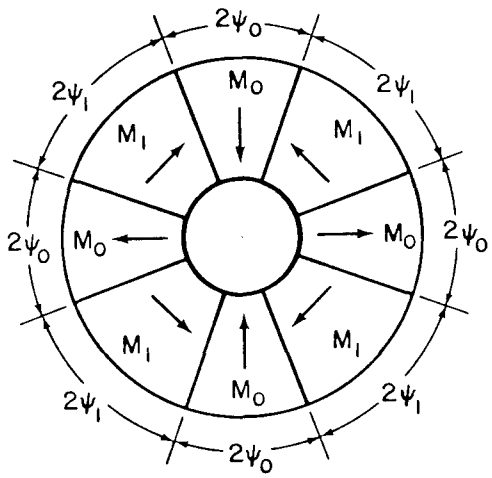

Fig. 3 Modified Eight Segment REC Quadrupole to Remove Sixth Harmonic Impurities

We shall assume $\mu_{\parallel} = \mu_{\perp} = 1$.

The general form for the multipole expansion of the scalar potential ϕ in the interior region is

$$\phi = \sum_{n=0}^{\infty} r^n e^{in\theta} \sum_j M_j e^{i(\alpha_j-(n+1)\theta_j)} \frac{1}{2\pi} \iint \frac{dxdy}{(x+iy)^{n+1}} \tag{4.1}$$

where α_j is the easy axis orientation of the j^{th} segment centered at azimuth θ_j, and where the integral is taken over the 2-D region of the j^{th} segment.

In the example shown in Figure 3, we have taken $\alpha_0 = 0$, $\alpha_1 = \frac{3\pi}{4}$, $\alpha_2 = \frac{3\pi}{2}$, $\alpha_3 = \frac{9\pi}{4}$, etc. It is easy to show that the multipoles n = 3, 4, 5, 7, 8, 9 vanish by symmetry and that the n = 6 multipole is given by

$$\phi_6 = \frac{4r^6}{7\pi a^5} \cos 6\theta (1 - (\frac{a}{b})^5)[M_0 \sin 7\psi_0 - M_1 \sin 7\psi_1] \tag{4.2}$$

The multipole field strength at the bore is therefore

$$B_6(a) = \frac{24}{7\pi} (1 - (\frac{a}{b})^5)[M_0 \sin 7\psi_0 - M_1 \sin 7\psi_1] \tag{4.3}$$

Similarly, the desired quadrupole field strength is given by

$$B_2(a) = \frac{8}{3\pi} (1 - \frac{a}{b})[M_0 \sin 3\psi_0 + M_1 \sin 3\psi_1] \tag{4.4}$$

If we have a material which has a linear B-H curve with $\mu_{\parallel} \neq \mu_{\perp}$, we can compensate for the sixth order multipole error by choosing ψ_0 and ψ_1 such that Equation (4.3) produces an equal and opposite n = 6 impurity.

If we wish to use different REC materials because of the need to guarantee linearity in the B-H curve into the 2nd and 3rd quadrants, we can similarly ensure the absence of the n = 6 harmonic by choosing

$$\frac{\sin 7\psi_1}{\sin 7\psi_0} = \frac{M_0}{M_1} \tag{4.5}$$

or

$$\tan[\frac{7}{2}(\psi_0 - \psi_1)] = -\frac{M_0-M_1}{M_0+M_1} \tan\frac{7\pi}{8} \simeq .414 \frac{M_0-M_1}{M_0+M_1} \tag{4.6}$$

As an example, if we take M_0 = 12.0 Kgauss (Material = S_mCo_5) and M_1 = 8.0 Kgauss (Material = $Sm_2(Co+TM)_{17}$), we are led to

$$\psi_0 = 23.18^0, \quad \psi_1 = 21.82^0 \tag{4.7}$$

in order to provide elimination of the n = 6 multipole.

V. Computer Model Calculations

The program PANDIRA[2] permits us to calculate the multipole fields for "real" magnet materials in any 2-D geometrical configuration with an arbitrary function for $B_{\parallel}(H_{\parallel})$ but with $\mu_{\perp}$ equal to a constant. We have performed the test calculations shown in the table to illustrate the effects of permeabilities different from unity, non-linear $B_{\parallel}(H_{\parallel})$ materials, and a two material configuration using the design principles for a compensated ring developed in Section IV.

These calculations were for the geometry shown in Figure 4 which is a flux plot for Case A with the ratio a/b = 1/3. This is one octant of an eight piece segmented ring with the pieces having an arc shape on the inside and trapezoidal shape on the outside. The form factor for the n^{th} field harmonic for this geometry, which is shown in Figure 5, is

$$\frac{\sin(n+1)\psi_0}{(n+1)\psi_0} - \left\{\frac{a}{b}\right\}^{n-1} \frac{\sin n\psi_0}{n\psi_0} \cos^n\psi_0 \tag{5.1}$$

For b=3a and n=2, there is only a 1% error if we use

$$\frac{\sin(n+1)\psi_0}{(n+1)\psi_0} \left\{1 - \frac{a}{b}\right\} \tag{5.2}$$

For n = 6, the second term in Equation (5.1) is completely negligible.

The table gives the results of the computations in terms of the strength of the fundamental quadrupole and the relative strengths of the multi-

[2] K. Halbach, R. F. Holsinger, "PANDIRA". "A Computer Program for the solution of Anisotropic Field Problems by a Direct Method," to be published.

pole field errors.

CASE - PIECES	(Kg) M_o	(Kg) M_1	ψ_o	ψ_1	$\mu_{o,\perp}$	$\mu_{1,\perp}$	$\mu_{\perp}$	(Kg) n = 2	% of n = 2 @ r = a n = 6	n = 10	n = 14	n = 18
A - 8	10	10	22.5°	22.5°	1.0	1.0	1.0	10.56	...	-22.6	...	12.6
B - 8	"	"	"	"	2.0	2.0	"	7.07	0.1	∿ "	1.4	∿ "
C - 16	10	10	22.5	22.5	1.0	1.0	1.0	12.63	...	...	...	12.5
D - 16	"	"	"	"	1.1	1.1	"	12.03	2.0	0.1	0.8	∿ "
E - 8	8	8	22.5	22.5	1.0	1.0	1.0	8.45	...	-22.6	...	12.6
F - 8	12	8	"	"	"	"	"	10.42	3.5	∿ "	2.2	∿ "
G - 8	"	"	23.2	21.8	"	"	"	10.43	0.2	∿ "	0.7	∿ "
H - 8	12	12	22.5	22.5	1.0	1.0	1.0	12.67	...	-22.6	...	12.6
I - 8	"	"	"	"	NON-LINEAR		1.0	11.29	0.1	-15.1	-2.0	7.3
J - 8	"	"	"	"	NON-LINEAR		1.0	9.39	5.8	-14.2	-4.3	6.9

In cases A-8 through D-16, harmonic errors due to μ_{11} different than unity are investigated. In case B-8, the fact that essentially no n = 6 error is produced even with an unrealistically high value of μ_{11} = 2 is surprising. The explanation is probably that the n = 6 term corresponds to Equation (3.9) which we expect is largely compensated by the N - 2 = 6 term which is present in an 8 section quadrupole. By contrast, in case D-16 the expected n=6 error is present for a realistic μ_{11}=1.1. In this case there is no compensating contribution from the 16 segment configuration.

Cases E-8 through G-8 show the effectiveness of the compensated ring design. In case F-8 a large n = 6 error results from $M_o \neq M_1$. It is essentially eliminated in Case G-8 by adjusting ψ_o and ψ_1 as prescribed in equations (4.5).

Finally in cases H-8 through J-8 we have calculated the errors due to truly nonlinear $B_{11}(H_{11})$ functions. In case I-8, $B_{11}(H_{11})$ is assumed linear into the second quadrant of the $B_{11}(H_{11})$ curve until approximately H_{11} = -9.5 K-Oersted. The material in case J-8 becomes nonlinear sooner at approximately H_{11} = -6.0 K-Oersted. The results show a significant decrease in quadrupole strength in addition to large non-allowed harmonic errors. It should also be noted that the allowed harmonics n = 10 and n = 18 change significantly. This would certainly be a source of error if they had been compensated for in the original configuration.

VI. Application of the Compensated Ring Design

A particular example where the compensated ring design may be applied is for REC quadrupole designs being considered for the final focus region of the Stanford Linear Collider (SLC) project[3].

[3]SLC Conceptual Design Report, SLAC-229, June 1980

One of the configurations for the final focus interaction region in the SLC is the so-called micro-quadrupole solution. A design concept for these micro-quadrupoles is shown in Figure 6. The unique requirements for these REC quadrupoles are the extremely high gradients of the order of 150 Kgauss/cm and the corresponding very small apertures of the order of 1 mm. These gradients may be achieved in principle, of course, since when an REC quadrupole is scaled down, the field strengths are unchanged and the gradient therefore is increased by the scale factor.

For the micro-quadrupole design, the maximum possible quadrupole strength is required since the very small aperture will be a difficult practical problem and the higher the strength, the larger the allowed aperture for a specified gradient. Therefore the compensated ring design would be most appropriate. Since, because of the small size, the volume of the material will be insignificant in the total cost, one would choose a very small ratio of a/b, e.g. a/b = 1/10. From Section II above, this ratio will require $B_{11}(H_{11})$ well into the third quadrant, i.e., linear to approximately - 1.8M.

A reasonable choice for the materials for the micro-quadrupole design would be a very high B_r material for the "M_o pieces" and very linear material for the "M_1 pieces." If we choose M_o = 12 Kgauss and M_1 = 8 Kgauss from commercially available materials, the micro-quadrupole design would have the following characteristics.

Bore radius, a = 1 mm
Outside radius, b = 10 mm
Quadrupole field at r = a, B_2 = 14.1 Kg
Quadrupole gradient, B_2' = 141 Kg/cm
Field allowed error,

field harmonic at r = a, $\frac{B_{10}}{B_2}$ = -22.6%

The very large value of this error field is not important from the micro-quadrupole application, since the beam size of a few microns is such a small fraction of the aperture.

VIII. Conclusion

We have shown that multipole impurities are introduced by REC materials with $\mu_{\parallel} \neq \mu_{\perp}$. We have shown that these impurities can be eliminated by choosing ψ_0 and ψ_1 to be slightly different from 22.5^{o}, and have confirmed this by the corresponding PANDIRA calculation.

We have also shown that multiple impurities are introduced by REC materials with non-linear B-H curves. These impurities can also be eliminated by choice of ψ_0 and ψ_1 appropriate to the M_0 and M_1 materials selected. This conclusion is confirmed by the corresponding PANDIRA calculation.

The techniques which have been outlined in this paper will also work for values of N higher than 8. The analysis is more complex, and it becomes necessary to choose $\alpha_j \neq 3\theta_j$ for some of the segments, but the results are similar to those obtained for the quadrupole with eight segments.

Similar techniques can also be used for the design of multipole magnets other than quadrupole.

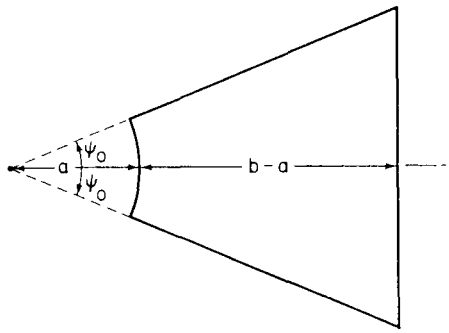

Fig. 5 Individual Segment with Interior Arc and Exterior Plan Surface

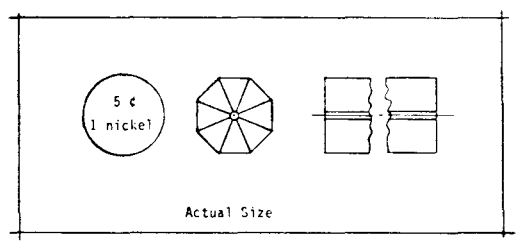

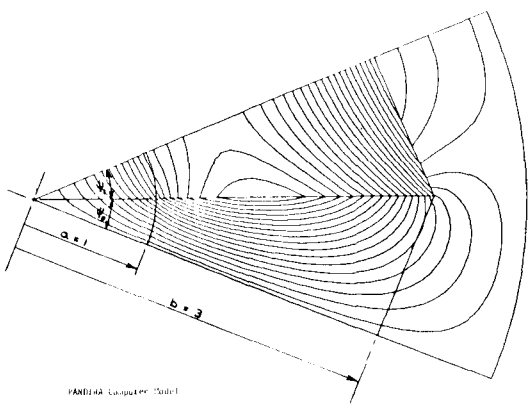

Fig. 4 Flux Plot for Eight Segment Quadrupole

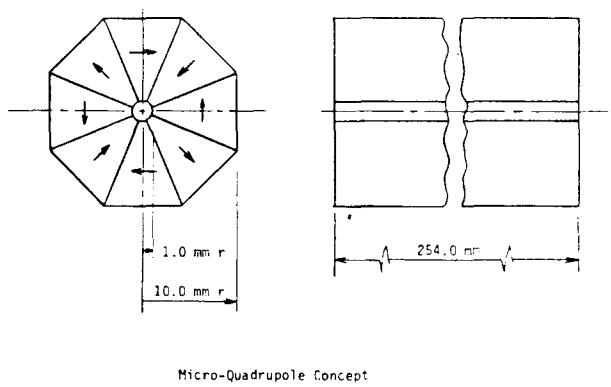

Fig. 6 Microquadrupole Design